Appendix L, Shasta Coldwater Pool Management

Attachment L.3 Winter-run Chinook Salmon Juvenile Production Index Model

L.3.1 Model Overview

Winter run Chinook salmon are unique in that they spawn in the late spring and summer when air temperatures are at seasonal highs and flows are at seasonal lows. Historically, this run migrated to higher elevation habitats where summer water temperatures were more appropriate for spawning and egg incubation. The only extant population is now restricted to spawning in the reach just below Keswick Dam. Although conditions below the dam are managed to support this run, there is concern that conditions during spawning and incubation may be reducing population productivity. To explore hypothesized relationships between juvenile winter run production and biological and environmental drivers we developed a model using the United States Fish and Wildlife Service (USFWS) winter run Chinook salmon juvenile production index (JPI) as the response variable.

The JPI is a standardized estimate of juvenile winter run passage at Red Bluff Diversion Dam. Juvenile Chinook salmon migrate past Red Bluff at various life stages and passage may occur days to months following emergence. The USFWS uses an assumed survival rate between the fry life stage and all-post fry life stages to standardize the estimate into “fry equivalents”. Potential predictor variables included metrics of flow, temperature and spawner abundance that were constructed to represent hypothesized relationships with productivity. Modeling was performed to identify the most explanatory flow and temperature metrics and then information theoretic methods were used to select best-approximating models.

Multi-model averaging led to the identification of two drivers that most affected juvenile winter run production; flow during incubation and emergence, and the number of female spawners. The predictive strength of flow is important because previous modeling efforts have focused on the effect of temperature on egg-to-fry survival, a calculation that uses the response used here (JPI) but with additional estimates and assumptions (Martin et al. 2017, Anderson et al. 2022). Neither of the previous studies have examined the effect of flow and have instead assumed non-temperature environmental effects were equal among all years.

L.3.2 Model Development

L.3.2.1 Methods

L.3.2.1.1 Data

Twenty-one years of data were used for this modeling (2002-2022). Data were available for 1996-1999; however, methods for the carcass survey and the specific population estimators used were not standardized until 2002. Juvenile data were not available for 2000 and 2001 due to a lack of sampling.

The response variable for this exercise was the winter run juvenile production index (JPI). The JPI is a standardized estimate of juvenile winter run passage at Red Bluff Diversion Dam. Juvenile Chinook salmon migrate past Red Bluff at various life stages and passage may occur days to months following emergence. The USFWS uses an assumed survival rate between the fry life stage and all-post fry life stages to standardize the estimate into "fry equivalents".

Independent variables were selected based on hypothesized drivers of variation in production and included both physical and biological factors (Table L.3-1). Three temperature variables were considered. The first two metrics were calculated at the station located on the Sacramento River at Highway 44 (CDEC station "SAC"). This location was selected because it is close to the midpoint of the winter run spawning habitat. Data from this station were not available in all years. When data were not available, it was interpolated using a linear model and values recorded at a station upstream (CDEC station "KWK") and a station downstream (CDEC station "CCR"). The two metrics calculated at this site were selected to represent both acute and chronic effects of temperature. The first metric was the average daily temperature between July 1st through September 30th. This period is when cold water pool is most likely to be limited and most eggs hatch by the end of September. This metric represents potential chronic effects of temperature on production across this period. The second metric is the number of degree days over 53°F (11.67°C) between May 1st and September 30th. This metric represents acute effects that occur once a threshold is exceeded while no effect occurs below that threshold. The value chosen for the threshold approximates values proposed as necessary to protect incubating eggs. The final temperature metric was the mean temperature at Red Bluff diversion Dam (CDEC station "RDB") during the peak month of juvenile winter run catch (October).

Four flow variables were considered, including: mean flow at Bend Bridge (CDEC station "BND") during incubation and emergence, mean flow at BND during the month of peak catch at Red Bluff, and the coefficient of variation in flow at BND during the month of peak catch at Red Bluff.

The estimated number of female winter-run spawners was also considered as a biological explanatory variable.

Table L.3-1. Environmental variables considered for modeling variation in JPI with a description, period represented and hypothesized relationship to JPI.

Covariate Name	Metrics description	Months	Hypothesis
Temp_SAC_I	Average temperature during key incubation period (Jul-Sep) at Hwy 44 (SAC). Indexes average temperature experienced by incubating eggs	July-September	Temperature effects on survival are primarily chronic and increase linearly with mean daily values in the period when cold water volume is limiting.
CD_above_11.67_I	Cumulative degrees per day above 11.67C during incubation period at Hwy 44 (SAC). Indexes magnitude of exposure to temperature stress	July-September	Temperature effects on production are primarily acute and occur when a threshold value is exceeded
Temp_RB_M	Mean temp @ Red Bluff during month of peak migration. Indexes metabolic demand of juveniles and their predators	October	Higher temperatures during rearing/migration increase predation intensity and demand for prey
Flow_IE	Mean flow at Bend Bridge during incubation and emergence.	May-October	Mortality effects of flow occur at daily time steps during incubation and emergence
Total_discharge_IE	Cumulative discharge at Bend Bridge (m3) during incubation and emergence	May-October	Mortality effects of flow occur at a seasonal time step in response to the total volume of water discharged during incubation and emergence
Flow_M	Mean flow at Bend Bridge during month of peak migration	October	Survival during migration is directly proportional to flow magnitude
Flow_CV_M	CV of flow at Bend Bridge during peak month of migration	October	Flow pulses increase survival (Hassrick et al. 2022)

L.3.2.1.2 Modeling and Analysis

We employed several methods to identify and analyze potential factors associated with observed JPI. First, we created exploratory scatter plots to visually assess the relationship between potential factors and JPI. Then we examined the correlation of these factors, and noted several highly correlated pairs (e.g., Flow_IE and Total_Discharge_IE Pearson's correlation > 0.99, see Table L.3-2).

To refine our list of potential factors, we created a Lasso model to highlight the important variables among the potential factors (McNeish 2015). Through regularization, Lasso models consider penalization for the number of included parameters within the modeling itself, as opposed to post hoc comparisons. Because of this, LASSO models perform well when the number of predictors exceeds the sample size or when strong correlations exist among predictors (multicollinearity). Unlike stepwise selection, LASSO models are not running multiple tests, and do not need Bonferroni corrections, and are less likely to be overfit due to “data dredging” than a stepwise procedure. Similarly, they are not sensitive to variable naming or order since everything is considered at once. Finally, LASSO model output contains quantitative measures of variable importance that are easy to interpret and extend to other analyses. Overall, LASSO models do a good job of highlighting factors most useful for prediction while accounting for correlated factors.

Based on the results of the LASSO model, and potential for managerial control of independent variables, we selected a set of a priori models to test. JPI is an integer count that is likely well modeled using a count process. Because the JPI data are over-dispersed, with variance significantly higher than the mean, we chose to model the process using negative binomial regression, with a square root link function that adequately accounts for the over-dispersion while still allowing for easy interpretation (as opposed to quasi- methods).

Models were compared using Bayesian Information Criterion (BIC) scores to determine how well models were supported by the data while not being overfit. BIC was selected due to the low number of data points and AIC’s propensity for over fitting with small sample sizes. The model with the lowest BIC score was designated as the “best fit model” and the BIC value of each candidate model was subtracted from the BIC value of the best fit models to calculate the ΔBIC value. Models, with ΔBIC values ≤5.0 were considered competing and BIC model weights were used to calculate model averaged coefficients and unconditional confidence interval. Additionally, leave one out cross validation (LOOCV) was used to estimate R^2 as measure of fit for individual models.

Finally, we created a prediction plot to compare the selected model’s predictions to the observed JPI values. These plots allow us to assess the accuracy of the model in predicting JPI based on the selected variables, and help highlight additional trends in predictions / residuals. All analysis was run in R (R Core Team 2023) with Lasso models coming from the glmnet package (Friedman et al 2010)

Table L.3-2. Pearson product-moment correlations between explanatory variables considered for use in modeling the winter run Chinook Salmon JPI.

	Temp_RB_M	**Flow_M**	**Flow_CV_M**	**Flow_IE**	**Total_discharge_IE**	**Temp_SAC_I**	**DD_above_11.67**
Temp_RB_M	1						
Flow_M	-0.382	1					
Flow_CV_M	0.214	0.369	1				
Flow_IE	-0.457	0.692	-0.053	1			
Total_discarge_IE	-0.459	0.695	-0.051	>0.99	1		
Temp_SAC_I	0.906	-0.378	0.258	-0.626	-0.627	1	
DD_above_11.67_I	0.888	-0.312	0.344	-0.605	-0.606	0.968	1

L.3.2.2 Assumptions / Uncertainty

The monitoring data analyzed here, and by Martin et al. (2017) and Anderson et al (2022), are not collected in a way that specific life stages (egg, fry, parr and smolts) can be separated for analysis of life stage-specific effects. Thus, there remains uncertainty as to the specific drivers affecting individual life stages that contribute to JPI. Field experiments that can elucidate life stage-specific drivers and thresholds are needed to develop a more granular understanding and ultimately to improve the effectiveness of management actions intended to improve spawning success and juvenile production of winter-run Chinook salmon.

L.3.2.3 Code and Data Repository

Code is available at: GitHub - fishsciences/2022-shasta_winter_run_survival-Public

Analysis files for the WR JPI input data and WR JPI analysis are available upon request.

L.3.2.4 Model Development Results

Exploratory plots showcase a strong relationship between JPI and Females, but also strong relationships with flow metrics, and weaker relationships coming from the temperature factors (Figure L.3-1).

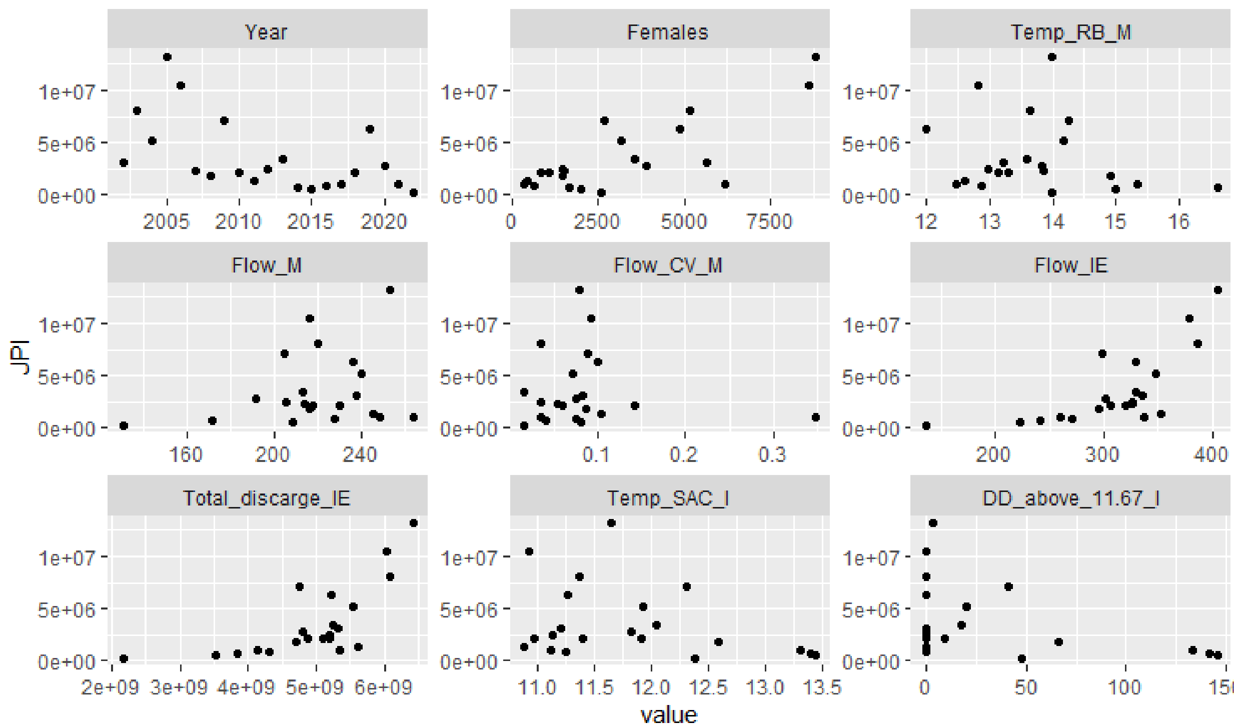

Figure L.3-1. Exploratory scatter plots comparing JPI to potential factors.

The Lasso model showed most support for including *Females*, *Flow_IE*, and *Flow_CV_M*. Out of the temperature metrics, *Temp_SAC_I* had the highest support. Seven candidate models were constructed using these variables and evaluated for relative fit as described above (Table L.3-3). Three of these models had good support in the data according to their Δ BIC scores (M1, M2, M4). These models explained between 78% and 74% of the total variation in JPI (Table L.3-3). All three competing models were used to calculate model averaged coefficients and unconditional confidence intervals for each variable (Table L.3-4). Coefficients with unconditional confidence intervals that did not include zero were considered to have good support in the data (Burnham and Anderson 2002).

Table L.3-3. Model selection results. Delta BIC is calculated using model 4 as baseline and R^2 values were calculated using leave-one-out cross validation.

Model	**Number of Parameters**	**BIC**	**ΔBIC**	**R^2**
1. Flow_IE + Temp_SAC_I + Flow_CV_M + Females	5	657.339	3.014	0.635
2. Flow_IE + Females	3	654.330	0.004	0.769
3. Flow_CV_M + Females	3	672.856	18.531	0.186
4. Flow_IE, Flow-CV-M + Females	4	654.325	0.00	0.639
5. Temp_SAC_I + Females	3	669.202	14.876	0.613
6. Temp_SAC_I + Flow_CV_M + Females	4	671.468	17.143	0.325
7. Flow_IE + Temp_SAC_I + Females	4	657.249	2.924	0.757

Table L.3-4. Model averaged parameters and unconditional 95% confidence intervals calculated using the four top models selected with BIC.

	Estimate	**Lower CI**	**Upper CI**
Intercept	-912	-1474	-332
Females	0.179	0.101	0.265
Flow_IE	6.656	5.133	7.993
Flow-CV-M	-2730	-4652	323
Temp_SAC_I	-25.443	-88.533	180.422

Model averaging found that two independent variables were well supported by the data (unconditional confidence interval did not include zero). These were the number of female spawners and mean flow during the incubation and early emergence period (Table L.3-4). Both variables had a direct relationship with JPI. Two variables were not well supported including the coefficient of variation in flow during the peak month of passage at Red Bluff and mean water temperature at Highway 44 during incubation and emergence. Model averaged coefficients predicted JPI values which closely tracked observed JPI across years, with the largest deviation occurring in 2009 (Figure L.3-2).

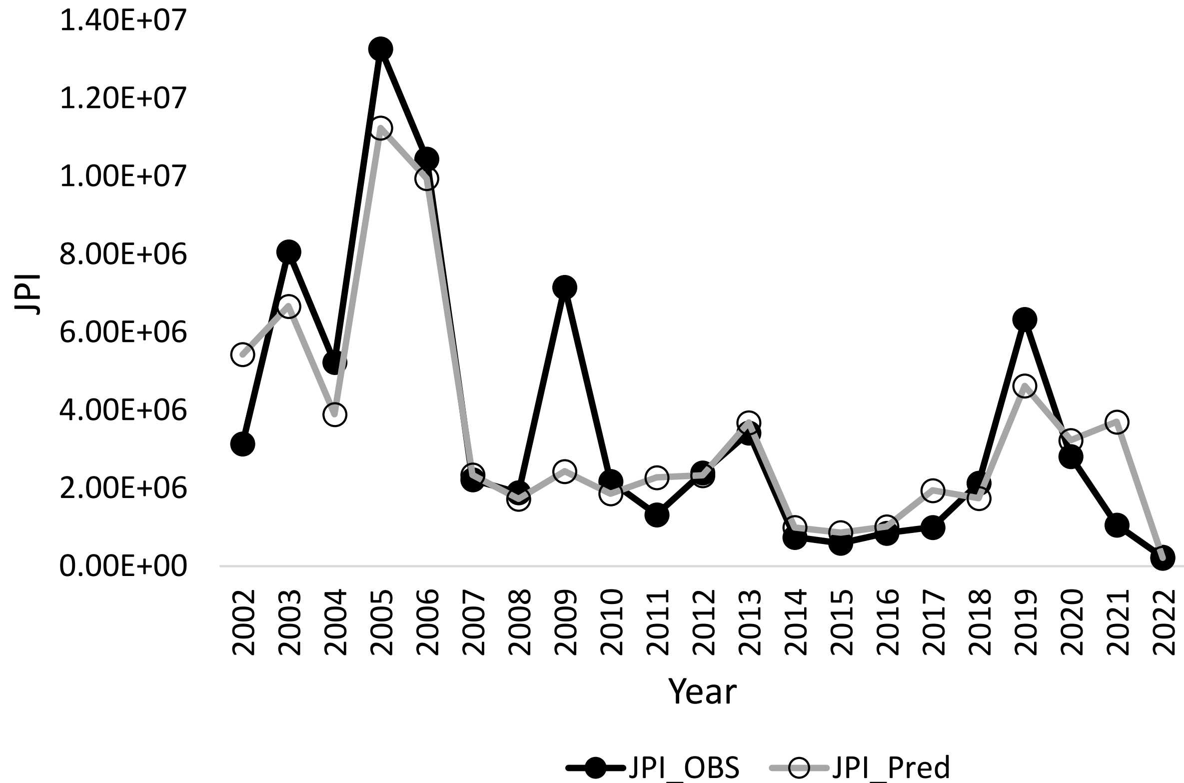

Figure L.3-2. Observed JPI values from 2002 to 2022 and predicted values using model averaged coefficients.

L.3.2.5 Model Development Discussion

Model selection and multi-model averaging identified the number of female spawners and flow during incubation and emergence as the two best supported predictors of juvenile winter run production. Both variables are well supported in the literature with a long history of research on the relationship between spawner abundance and juvenile recruitment (Subbey et al. 2014) and the effect of flow on juvenile production (e.g., Munsch et al. 2020). Thus, the importance of these variables was not surprising. Within the Sacramento River, previous modeling efforts have focused on the effect of temperature on egg-to-fry survival, a calculation that uses the response used here (JPI) but with additional estimates and assumptions (Martin et al. 2017, Anderson et al. 2022). Neither of the previous studies have examined the effect of flow and have instead assumed non-temperature effects were equal among all years. This analysis indicates that interannual variation in flow has a well-supported effect on juvenile winter-run production whereas the effect of temperature was not as well supported.

There has been considerable research on how temperature affects the survival of Chinook salmon eggs and strong effects have been identified (Beacham and Murray 1989, Geist et al. 2006). Thus, it may initially be surprising that temperature was not a strong driver in this analysis. However, operations of Shasta Reservoir are designed to help ensure temperatures in the spawning and egg incubation reach remain below levels where laboratory studies suggest rapidly increasing mortality will occur (USFWS 1999). Modeling by Martin et al. (2017) and Anderson et al. (2022), assume that temperature is the only interannual environmental driver of survival. The highest temperatures often occur in the lowest flow years. However, the effect of flow has not previously been tested, and the conclusion of the Martin et al. (2017) was that the threshold temperature must be lower in the field than what has been derived from laboratory studies. Martin et al. (2017) acknowledges that an alternative hypothesis to explain their findings is that some factor other than temperature is influencing interannual variation. This analysis provides strong evidence for this alternative hypothesis with flow enjoying stronger support than water temperature.

The monitoring data analyzed here, and by Martin et al. (2017) and Anderson et al (2022), are not collected in a way that specific life stages (egg, fry, parr and smolts) can be separated for analysis of life stage-specific effects. Thus, there remains uncertainty as to the specific drivers affecting individual life stages that contribute to JPI. Field experiments that can elucidate life stage-specific drivers and thresholds are needed to develop a more granular understanding and ultimately to improve the effectiveness of management actions intended to improve spawning success and juvenile production of winter-run Chinook salmon.

L.3.3 Model Application

For this effects analysis, the JPI model was run for years 2002-2022 when data on female spawners was available. Temperature data at node (BLW KESWICK) from the HEC-5Q model was used to represent the CDEC station SAC (Sacramento River at Highway 44). Flow data from Calsim 3 node (C_SAC257) was used to represent CEDC station BND (Sacramento River at Bend Bridge). Data from these nodes was summarized the same way as described in Table L.3-1 above. The output of the model is the predicted JPI for each year.

L.3.4 Results

L.3.4.1 BA

When grouped by water year type, the highest mean predicted JPI value occurred under NAA during above normal water years (4,166,909) and the lowest mean predicted JPI value occurred during above critical water years (1,084,428) under Alt2 With TUCP Without VA (Figure L.3-3 and Table L.3-5).

The highest predicted JPI value across all years occurred in 2005 under Alt2 Without TUCP Delta VA (8,901,808). The lowest JPI values occurred in 2014 under Alt2 With TUCP Without VA (202,083, Figure L.3-4 and Table L.3-6).

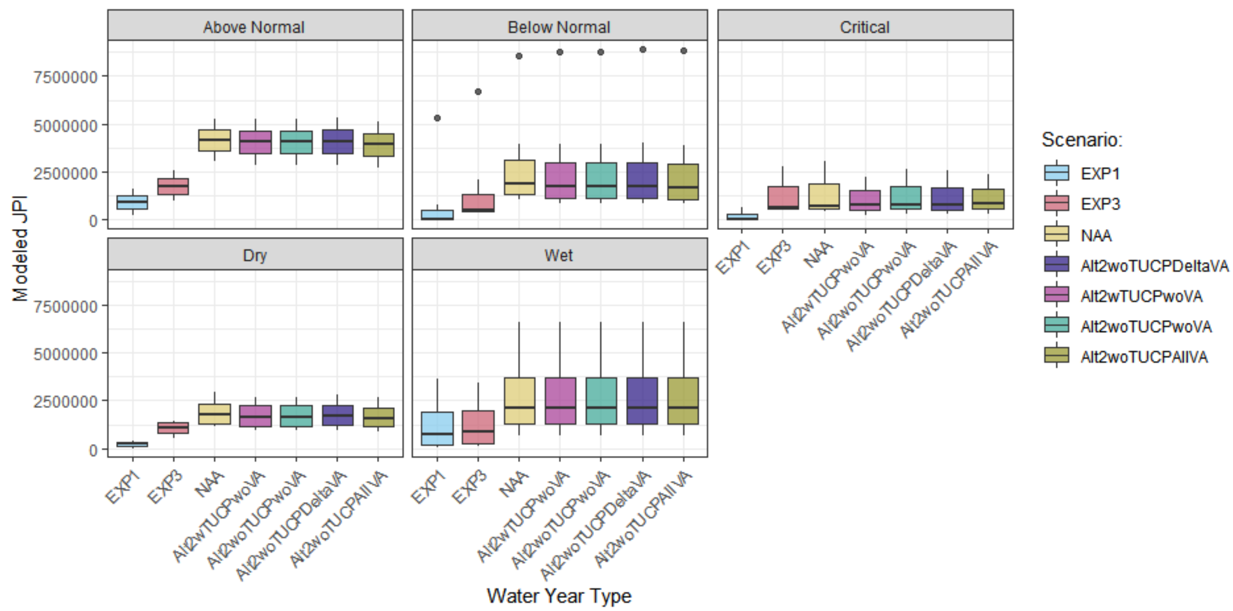

Figure L.3-3. Observed JPI values from 2002 to 2022 and predicted values under BA scenarios by water year type.

Table L.3-5. JPI observed and mean predicted values under BA scenarios from 2002 to 2022 by water year type.

Water Year Type	Observed JPI	NAA	EXP1	EXP3	Alt2 wTUCP woVA	Alt2 woTUCP woVA	Alt2 woTUCP DeltaVA	Alt2 woTUCP AllVA
Above Normal	6,652,583	4,166,909	938,222	1,767,935	4,064,905	4,064,717	4,080,225	3,927,614
Below Normal	3,743,451	2,903,175	898,043	1,595,262	2,792,077	2,792,278	2,814,852	2,761,983
Critical	799,585	1,413,014	221,555	1,326,659	1,084,428	1,250,915	1,215,117	1,163,048
Dry	3,820,593	1,903,154	211,001	1,055,059	1,750,491	1,751,186	1,788,049	1,675,850
Wet	4,776,674	2,874,042	1,311,624	1,344,053	2,864,663	2,864,578	2,864,874	2,864,352

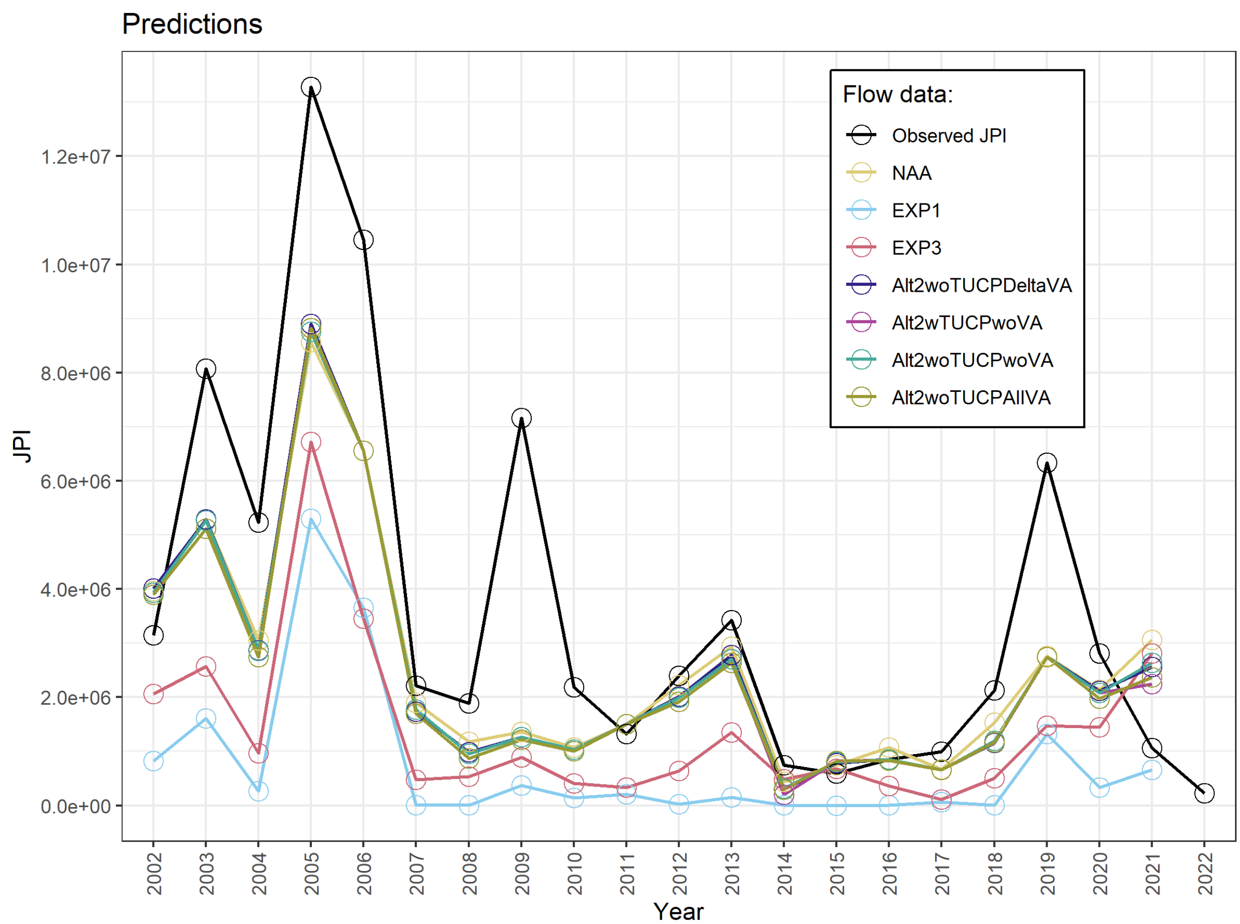

Figure L.3-4. Observed JPI values from 2002 to 2022 and predicted values under BA scenarios.

Table L.3-6. JPI observed and predicted values under BA scenarios from 2002 to 2021.

Year	Water Year Type	NAA	EXP1	EXP3	Alt2wTUCP woVA	Alt2woTUCP woVA	Alt2woTUCP DeltaVA	Alt2woTUCP AllVA
2002	Below Normal	3,959,028	818,025	2,060,195	3,933,154	3,932,752	4,009,544	3,892,211
2003	Above Normal	5,284,368	1,608,204	2,573,376	5,272,227	5,271,497	5,290,793	5,116,249
2004	Above Normal	3,049,451	268,240	962,493	2,857,582	2,857,937	2,869,657	2,738,979
2005	Below Normal	8,564,866	5,299,183	6,715,426	8,755,564	8,755,512	8,901,808	8,825,628
2006	Wet	6,559,160	3,658,496	3,453,628	6,558,389	6,558,386	6,558,363	6,558,368
2007	Below Normal	1,899,415	5,198	479,164	1,775,579	1,776,101	1,735,995	1,700,450
2008	Dry	1,173,361	3,191	533,031	960,493	960,380	982,025	872,844
2009	Dry	1,361,517	366,449	888,745	1,262,236	1,261,794	1,263,268	1,215,084
2010	Below Normal	1,071,971	135,590	412,359	1,035,097	1,035,100	1,035,352	1,000,173
2011	Wet	1,506,881	203,111	327,792	1,504,149	1,504,147	1,504,190	1,504,206
2012	Below Normal	2,225,736	23,626	636,031	1,992,567	1,994,803	2,008,791	1,917,065
2013	Dry	2,935,972	146,488	1,347,491	2,700,273	2,702,173	2,784,318	2,641,898
2014	Critical	436,339	2,333	490,476	202,083	311,402	301,173	298,193
2015	Critical	743,471	9	681,739	810,739	802,812	781,320	823,065
2016	Below Normal	1,069,988	1,720	358,538	854,396	853,181	849,861	835,011
2017	Wet	665,046	63,850	115,317	656,478	656,325	656,552	655,308
2018	Below Normal	1,531,224	2,956	505,122	1,198,182	1,198,497	1,162,616	1,163,344
2019	Wet	2,765,082	1,321,039	1,479,475	2,739,635	2,739,453	2,740,390	2,739,526
2020	Dry	2,141,768	327,876	1,450,968	2,078,964	2,080,396	2,122,583	1,973,576
2021	Critical	3,059,232	662,322	2,807,763	2,240,463	2,638,532	2,562,858	2,367,887

L.3.4.2 EIS

Under Alt1, the mean predicted JPI is generally higher than NAA, ranging from 45.23% higher in 2014 to 8.31% lower in 2003 (Table L.3-7, Figure L.3-5).

Under Alt2 with TUCP without VA, the mean predicted JPI is generally lower than NAA, ranging from 10.95% higher in 2015 to 53.08% lower in 2014.Under Alt2 without TUCP without VA, the mean predicted JPI is generally similar to NAA with an even number of years higher and lower than NAA, ranging from 272.52.98% higher in 2014 to 85% lower in 2017.Under Alt2 without TUCP Delta VA, the mean predicted JPI is generally lower than NAA, ranging from 4.45% higher in 2005 to 29.91% lower in 2014

Under Alt2 without TUCP Systemwide VA, the mean predicted JPI is generally lower than NAA, ranging from 3.60% higher in 2005 to 30.68% lower in 2014.

Under Alt3, the mean predicted JPI is generally lower than NAA, ranging from 39.30% higher in 2017 to 45.96% lower in 2018.

Under Alt4, the mean predicted JPI is generally lower than NAA, ranging from 5.90% higher in 2020 to 27.68% lower in 2014.

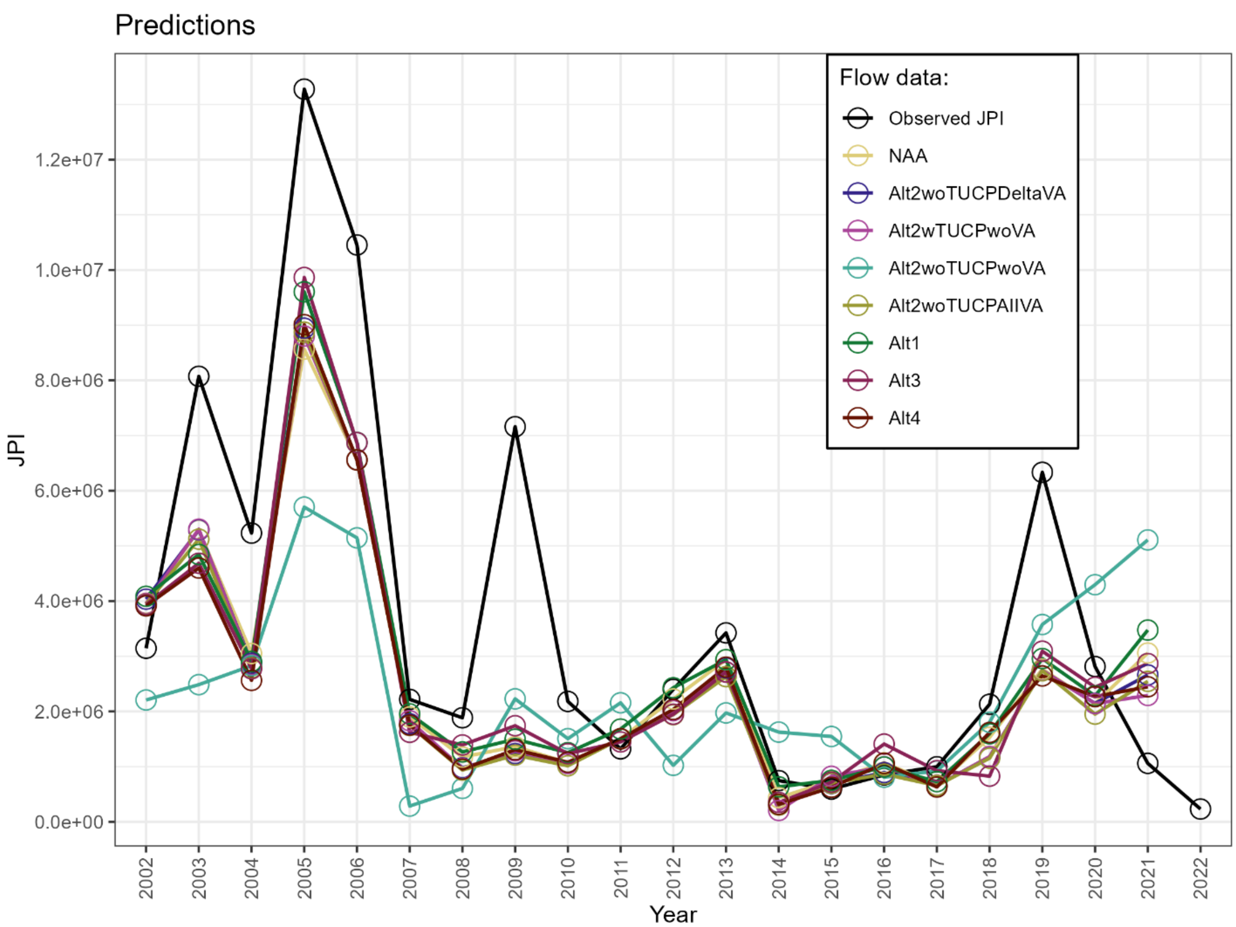

Figure L.3-5. Observed JPI values from 2002 to 2022 and predicted values under EIS scenarios.

Table L.3-7. JPI observed and predicted values under EIS scenarios from 2002 to 2021

Year	NAA	Alt1	Alt2wTUCP woVA	Alt2woTUCP woVA	Alt2woTUCP DeltaVA	Alt2woTUCP AllVA	Alt3	Alt4
2002	3959027.985	4086931.7 (3.23%)	3956028.3 (-0.08%)	2207140 (-44.25%)	4034274 (1.9%)	3943246.3 (-0.4%)	3936133.7 (-0.58%)	3912864.1 (-1.17%)
2003	5284368.415	4845104.2 (-8.31%)	5303741.7 (0.37%)	2485514.1 (-52.96%)	5290840.9 (0.12%)	5122851.9 (-3.06%)	4685515.4 (-11.33%)	4599483.1 (-12.96%)
2004	3049450.569	2905758.8 (-4.71%)	2846128.6 (-6.67%)	2828438.8 (-7.25%)	2873615.1 (-5.77%)	2787569.4 (-8.59%)	2772694.2 (-9.08%)	2562879.5 (-15.96%)
2005	8564865.603	9604400.7 (12.14%)	8802211.7 (2.77%)	5703602.9 (-33.41%)	8945918.5 (4.45%)	8873627.9 (3.6%)	9864235.1 (15.17%)	9009385.8 (5.19%)
2006	6559160.304	6874386.7 (4.81%)	6558430.5 (-0.01%)	5145443.3 (-21.55%)	6558377.7 (-0.01%)	6558324 (-0.01%)	6871630.9 (4.76%)	6558890.5 (0%)
2007	1899415.337	1955999.6 (2.98%)	1830915.2 (-3.61%)	284929.1 (-85%)	1775922.6 (-6.5%)	1745868 (-8.08%)	1622190.2 (-14.6%)	1752644.6 (-7.73%)
2008	1173361.363	1266288.2 (7.92%)	965563 (-17.71%)	604527.4 (-48.48%)	978681.9 (-16.59%)	937510.5 (-20.1%)	1392213.4 (18.65%)	954725.1 (-18.63%)
2009	1361516.834	1496967 (9.95%)	1285722.2 (-5.57%)	2227882.3 (63.63%)	1237024.2 (-9.14%)	1208314.7 (-11.25%)	1740691.7 (27.85%)	1306137.8 (-4.07%)
2010	1071971.475	1252799.9 (16.87%)	1054805.8 (-1.6%)	1506087.2 (40.5%)	1062681.3 (-0.87%)	1014839.8 (-5.33%)	1234426.1 (15.15%)	1079547.4 (0.71%)
2011	1506880.925	1681186.2 (11.57%)	1504108.4 (-0.18%)	2156486.8 (43.11%)	1504117.9 (-0.18%)	1504146.6 (-0.18%)	1447667.9 (-3.93%)	1504264 (-0.17%)
2012	2225735.614	2429711.6 (9.16%)	2015850.1 (-9.43%)	1022840.2 (-54.04%)	2023205 (-9.1%)	1941662 (-12.76%)	1949139.3 (-12.43%)	2036282.1 (-8.51%)
2013	2935971.557	2938987.1 (0.1%)	2717202.9 (-7.45%)	1973000.2 (-32.8%)	2788836.9 (-5.01%)	2630668.7 (-10.4%)	2713940.1 (-7.56%)	2802951.1 (-4.53%)

Year	NAA	Alt1	Alt2wTUCP woVA	Alt2woTUCP woVA	Alt2woTUCP DeltaVA	Alt2woTUCP AllVA	Alt3	Alt4
2014	436338.9637	633704.7 (45.23%)	204716.1 (-53.08%)	1625456.6 (272.52%)	305846.3 (-29.91%)	302468.6 (-30.68%)	351365 (-19.47%)	315549.8 (-27.68%)
2015	743471.4595	751759.8 (1.11%)	824874 (10.95%)	1546391.8 (108%)	693295.8 (-6.75%)	698065.2 (-6.11%)	718351.1 (-3.38%)	624328.5 (-16.03%)
2016	1069988.494	993376.5 (-7.16%)	996050.8 (-6.91%)	807761.5 (-24.51%)	892534.7 (-16.58%)	863143.1 (-19.33%)	1408894 (31.67%)	1059016 (-1.03%)
2017	665045.8628	728054.4 (9.47%)	656435.9 (-1.29%)	921416.8 (38.55%)	656582.6 (-1.27%)	655508.5 (-1.43%)	926410.6 (39.3%)	630336.9 (-5.22%)
2018	1531223.672	1595583.4 (4.2%)	1181949.9 (-22.81%)	1803554.9 (17.79%)	1177801.3 (-23.08%)	1152991.8 (-24.7%)	827462.3 (-45.96%)	1618826.5 (5.72%)
2019	2765081.534	2958158.1 (6.98%)	2742245.7 (-0.83%)	3575680.1 (29.32%)	2742350.3 (-0.82%)	2738325.2 (-0.97%)	3091360 (11.8%)	2643601.5 (-4.39%)
2020	2141768.12	2281827.5 (6.54%)	2142056.6 (0.01%)	4297050.9 (100.63%)	2145643.7 (0.18%)	1951396.9 (-8.89%)	2439424.6 (13.9%)	2268027.4 (5.9%)
2021	3059232.437	3474810.2 (13.58%)	2290432.4 (-25.13%)	5108254.4 (66.98%)	2661664.8 (-13%)	2545931.6 (-16.78%)	2867744.2 (-6.26%)	2447288.5 (-20%)

L.3.5 References

Anderson, J.J., W.N. Beer, J.A. Israel, and S. Greene. 2022. Targeting River operations to the critical thermal window of fish incubation: model and case study on Sacramento River winter-run Chinook salmon. *River Research and Applications* 38:895-905.

Beacham, T.D., Murray, C.B. 1989. Variation in developmental biology of sockeye salmon (*Oncorhynchus nerka*) and Chinook salmon (*O. tshawytscha*) in British Columbia. *Canadian Journal of Zoology* 67:2081-2089.

Burnham KP, Anderson DR. 2002. Model Selection and Multimodel Inference: Practical Information-theoretic Approach (2nd edn). Springer-Verlag: New York.

Geist, D.R., Abernethy, C.S., Hand, K.D., Cullinan, V.I., Chandler, J.A., Groves, P.A. 2006. Survival, development, and growth of fall Chinook salmon embryos, alevins, and fry exposed to variable thermal and dissolved oxygen regimes. *Transactions of the American Fisheries Society* 135:1462-1477.

Jerome Friedman, Trevor Hastie, Robert Tibshirani (2010). Regularization Paths for Generalized Linear Models via Coordinate Descent. *Journal of Statistical Software*, 33(1), 1-22. URL https://www.jstatsoft.org/v33/i01/.

Martin, B.T., Pike, A., John, S.N., Hamda, N., Roberts, J., Lindley, S. & Danner, E.M. 2017. Phenomenological vs. biophysical models of thermal stress in aquatic eggs. *Ecology Letters* 20:50-59.

McNeish, D.M. 2015. Using Lasso for predictor selection and to assuage overfitting: a method long overlooked in behavioral sciences. Multivariate Behavioral Research 50:471-483.

Munsch, S., C. Greene, R. Johnson, W. Satterthwaite, H. Imaki, P. Brandes and M. O'Farrell. 2020. Science for integrative management of a diadromous fish stock: interdependencies of fisheries, flow, and habitat restoration. *Canadian Journal of Fisheries and Aquatic Sciences*. 77. 10.1139/cjfas-2020-0075.

R Core Team (2023). *R: A language and environment for statistical computing.* R Foundation for Statistical Computing, Vienna, Austria. URL https://www.R-project.org/

Subbey, S., Devine, J.A., Schaarschmidt, U., Nash, R.D.M. 2014. Modelling and forecasting stock-recruitment: current and future perspectives. *ICES Journal of Marine Science* 71:2307-2322.

USFWS 1999. *Effect of temperature on early-life survival of Sacramento River fall- and winter-run Chinook Salmon.* U.S. Fish and Wildlife Service Report, Northern Central Valley Fish and Wildlife Office Red Bluff, California

L.3.6 Supplemental Materials

L.3.6.1 Lasso modeling

Justification for using Lasso modeling for variable selection prior to BIC-based model selection

Compared to Repeated BIC, LASSO models:

- Handles multicollinearity
- Perform well when the number of predictors exceeds the sample size or when strong correlations exist among predictors.
- Creates quantitative measures of variable importance. Easy to interpret or extend to other models.
- Repeatable. Output does not depend on variable names or order they were entered.
- No data dredging. Stepwise selection is prone to overfitting with small data sets. Does not need to be adjusted for multiple tests (Bonferroni corrections).

L.3.6.2 Predictive plots for competing models (1,2,4, and 7) identified in the model selection process based on BIC values.

Below are predictive plots for the four competing models identified using BIC (Models 1, 2, 4, and 7). It should be noted that when using information theoretic methods there is little support for selecting a single model among those that found to be competing with Δ BIC values and model weights. In this case, model averaging is recommended to integrate the information available from all the competing models. Thus, it would not be appropriate to interpret one competing model to the exclusion of the others.

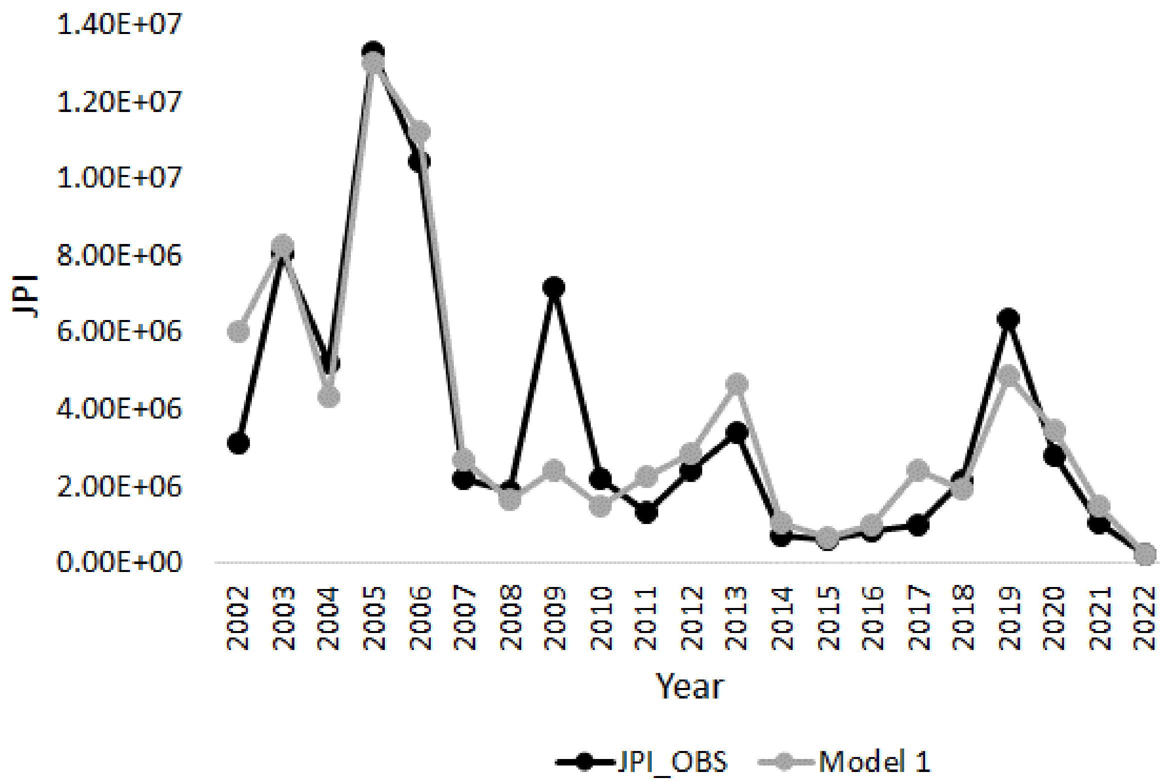

Figure L.3-6. Observed JPI and Model 1 predictive JPI, by year (2002 - 2022).

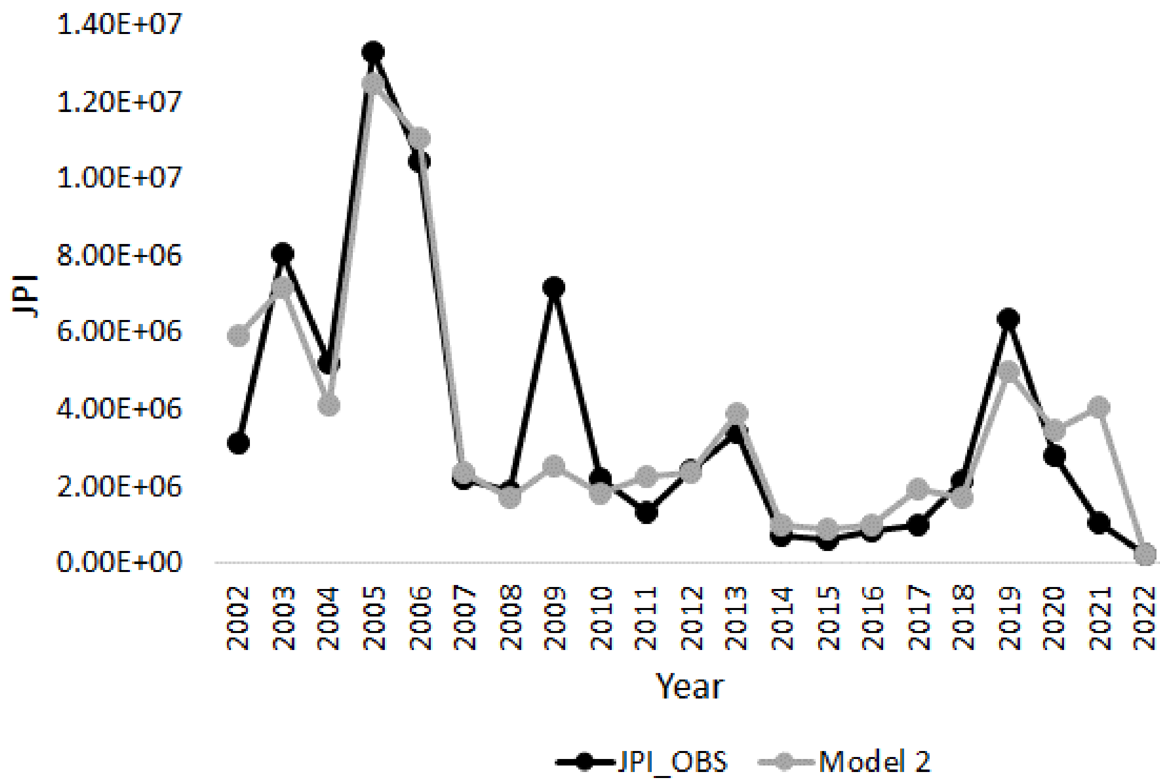

Figure L.3-7. Observed JPI and Model 2 predictive JPI, by year (2002 - 2022).

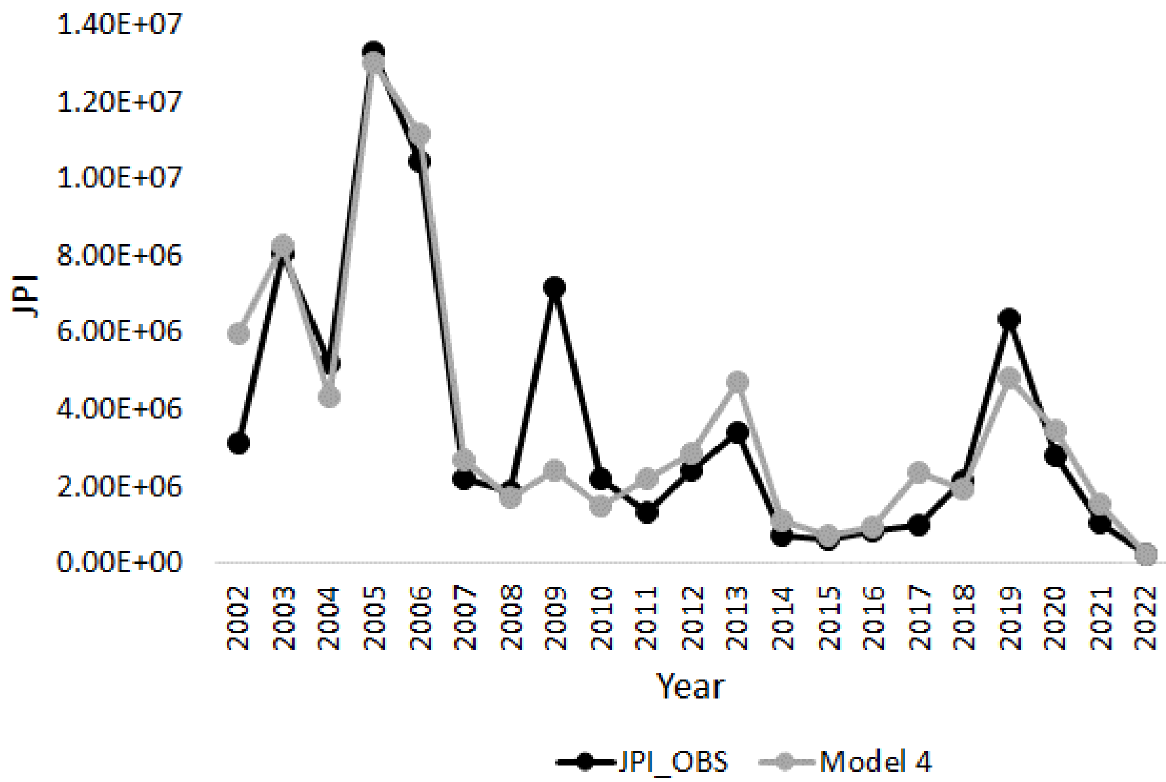

Figure L.3-8. Observed JPI and Model 4 predictive JPI, by year (2002 - 2022).

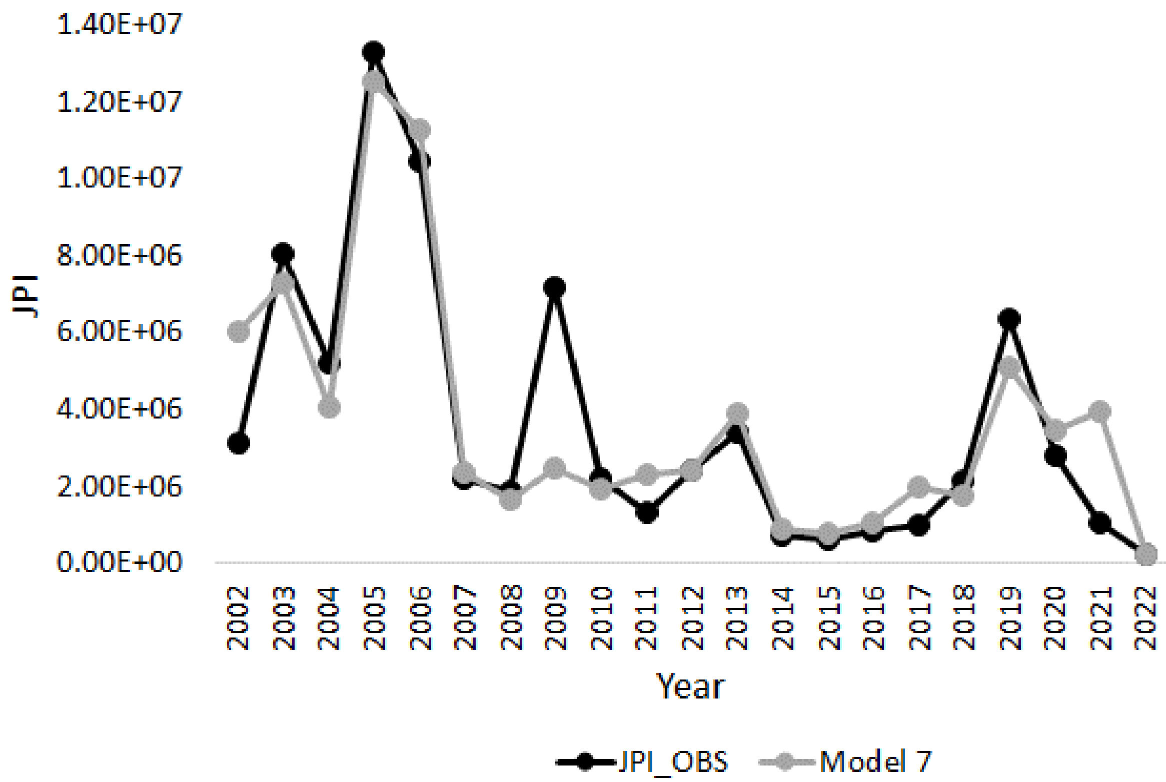

Figure L.3-9. Observed JPI and Model 7 predictive JPI, by year (2002 - 2022).